Phase behavior of disklike hard-core mesogens

J. A. C. Veerman* and D. Frenkel
FOM—Institute for Atomic and Molecular Physics, Kruislaan 407, 1098 SK Amsterdam, The Netherlands
(Received 4 December 1991)

We report a computer-simulation study of a system of "hard cut spheres," oblate particles that are obtained by slicing off the top and bottom caps of a sphere at a distance $L/2$ from the equatorial plane. This system serves as a model for a disklike mesogen. The phase behavior of this system is found to be strongly dependent on the length-to-width ratio (L/D) of the particles. In addition to isotropic and solid phases, we find nematic and columnar phases for $L/D=0.1$. For $L/D=0.2$ we find a columnar phase, and a phase with cubic orientational order but no translational order. For $L/D=0.3$, only the isotropic fluid and the solid are stable. Where possible, we have located the phase transitions.

PACS number(s): 61.20.Ja, 64.70.Md, 05.70.Fh, 61.30.By

I. INTRODUCTION

Computer simulation has proved to be a useful tool to gain a better understanding of the relation between the macroscopic and microscopic properties of liquid-crystalline materials. In some cases, fundamental questions about the factors that determine the formation of mesophases could be answered by simulations on very simple model systems, in which the molecules interacted only through hard-core repulsion [1]. Among other things, such simulations have shown that attractive interactions are not required for the formation of a smectic liquid crystal [2].

The majority of liquid-crystal simulations to data have dealt with rodlike molecules. However, in a number of simulations disk-shaped molecules were studied, in particular platelets [3] and oblate ellipsoids [4,5]. A closely related model was used by Siders and co-workers in the study of monolayers of disklike molecules [6]. However, the three-dimensional model systems studied in Refs. [3,4,5] apparently do not form liquid-crystalline phases other than the nematic phase. Such behavior is plausible if one considers the limiting case of a perfectly aligned nematic phase of disklike molecules. In the system of infinitely thin platelets considered in Ref. [3], the excluded volume vanishes once the particles are perfectly aligned. In that case, there is no driving force to form other liquid-crystalline phases. For the ellipsoid system used in Ref. [4], a perfectly aligned nematic phase is equivalent to a hard-sphere fluid, as can be seen by an affine transformation of the coordinate along the nematic director. Obviously, in such a system, additional liquid-crystalline phases are excluded.

In the present paper, we report the results of extensive simulations on a model system of disklike particles to which the above arguments do not apply. As a consequence, we may expect to find liquid-crystalline phases other than nematic in this system. The model system that we have considered consists of so-called "cut spheres" (see Fig. 1). A cut sphere is defined as follows. Consider a sphere with diameter D. Now remove those parts of the sphere that are more than $\frac{1}{2}L$ above or below the equatorial plane. What remains is a disklike object with flat caps and spherical rims. The "flatness" of the cut sphere is determined by the aspect ratio L/D, where L is the height of the particle in the direction perpendicular to the equatorial plane. Unlike the platelets studied in Ref. [3], cut spheres have a finite excluded volume even when they are perfectly aligned. Moreover, unlike the ellipsoid system, an assembly of aligned cut spheres cannot be mapped on a hard-sphere system. From a computational point of view, cut spheres have certain advantages over other models for disklike molecules such as short cylinders [7] and oblate spherocylinders [8]. Most importantly, the test for overlap between two cut spheres can be carried out in a finite number of steps. In contrast, in the simulations of oblate spherocylinders in Ref. [8] the overlap test included an iterative search procedure. The test for overlap between hard cylinders should be rather similar to the oblate spherocylinder case.

It is known from experiment [9] that systems of disklike molecules can form a variety of liquid-crystalline phases, most notably a columnar phase. Preliminary results of our numerical study of an assembly of cut spheres indicated that a columnar phase may indeed form in the cut-sphere system [10,11]. However, it is known from a systematic study of the phase behavior of hard, parallel spherocylinders that the periodic boundary conditions in small systems may, in some cases, induce spurious columnar order [12]. It is therefore important to check wheth-

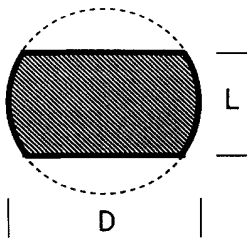

FIG. 1. Side view of a cut sphere with diameter D and thickness L.

er or not the columnar ordering in a system of cut spheres is stable as the system size is increased. In the present more extensive study we provide evidence that a stable columnar phase is indeed formed in systems of sufficiently flat cut spheres. For $L/D=0.1$, this phase coexists with a nematic phase. Surprisingly enough, for values of L/D larger than ~ 0.2, the nematic phase is not present. Instead a phase with extended cubic orientational order and no translational order is observed. We denote this phase "cubatic," in order to distinguish it from a cubic phase, which does have translational order. To our knowledge, cubatic orientational ordering in molecular systems has been observed neither experimentally nor, for that matter, in earlier simulations.

II. SIMULATIONS: GENERAL ASPECTS

A. System preparation and equilibrium

We have performed *Nvt* Monte Carlo (MC) simulations on systems of cut spheres with aspect ratio $L/D=0.1$, 0.2, and 0.3, using periodic boundary conditions. In all cases, we performed both expansion runs, starting from the close-packed crystal (see below) and compression runs, starting from the dilute-gas phase or, in some cases, some other well-equilibrated-state point. In the simulations of the $L/D=0.1$ system, we considered systems of 256 and 288 particles in the isotropic and nematic phases, and 576 particles in the columnar and crystalline phases. For reasons described in Secs. IV and V below, most of the simulations of cut spheres with $L/D=0.2$ and 0.3 were performed on larger systems: $N=1728$ and 2048 for $L/D=0.2$ and $N=2048$ for $L/D=0.3$, where N denotes the number of particles. Preceding all production runs of the high-density crystal and columnar phases and of the phase with cubic orientational order, we allowed the system to equilibrate at constant volume after every expansion or compression. During this equilibration, the simulation box was allowed to change its shape, in order to relieve possible stresses in the system. In all cases we did, however, keep the simulation box rectangular. In the simulations of the (low-density) isotropic and nematic phases, the shape of the simulation box was always kept fixed. Further details about the runs are given in Secs. III–V.

The initial shape of the simulation box was chosen to be compatible with the crystal structure of a closed-packed lattice of cut spheres. In fact, there are at least two distinct close-packed structures of the cut-sphere system. In the limit $L/D\rightarrow 1$ (hard spheres), one structure reduces to the well-known face-centered-cubic (fcc) structure, and the other to the hexagonal-close-packed (hcp) structure. In our simulations, we have used the latter solid structure as our initial configuration. For hard-sphere crystals it is known that the difference in stability between the fcc and hcp phases (if any) is very small [13]. We assume that the same holds for the relative stability of the different close-packed structures of the cut-sphere crystal. In the close-packed structure that we used as the starting configuration in our simulations, the crystal unit cell contains four cut spheres, all with their axes parallel to the z direction. The coordinates of the four particles in the crystal unit cell are

$$
\begin{aligned}
&\mathbf{r}_1=(0,0,0)\ ,\\
&\mathbf{r}_2=\left(\tfrac{1}{2}\sqrt{4-(L/D)^2},0,\tfrac{1}{2}L/D\right)\ ,\\
&\mathbf{r}_3=\left[\frac{1}{2}\frac{2-(L/D)^2}{4-(L/D)^2}\sqrt{4-(L/D)^2},\left[\frac{3-(L/D)^2}{4-(L/D)^2}\right]^{1/2},\tfrac{1}{2}L/D\right]\ ,\\
&\mathbf{r}_4=\left[\left[\frac{1}{2}+\frac{1}{2}\frac{2-(L/D)^2}{4-(L/D)^2}\right]\sqrt{4-(L/D)^2},\frac{1}{2}\left[\frac{3-(L/D)^2}{4-(L/D)^2}\right]^{1/2},0\right]\ ,
\end{aligned}
\tag{1}
$$

where we have used the diameter D of the cut spheres as our unit of length. The packing fraction of this close-packed (CP) structure is given by

$$\eta_{\mathrm{CP}}=\frac{\pi}{6}[3-(L/D)^2]^{1/2}\ . \tag{2}$$

Note that for $L/D=1$ (hard spheres), Eq. (2) reproduces the known result $\eta_{\mathrm{CP}}=\pi/\sqrt{18}$, while for $L/D\rightarrow 0$ the result for hard disks is recovered: $\eta_{\mathrm{CP}}=\pi/\sqrt{12}$. As v_0, the volume of a single cut sphere equals $(\pi/12)D^3(L/D)[3-(L/D)^2]$, the number density at regular close packing is given by

$$\rho_{\mathrm{CP}}=\frac{2(D/L)}{[3-(L/D)^2]^{1/2}}\ . \tag{3}$$

B. Structural probes

The detection of different kinds of orientational and translational order in a computer simulation requires special care. For instance, the structural information that is contained in the familiar radial distribution function $g(r)$ is insufficient to distinguish between different kinds of (liquid-) crystalline ordering. Hence, other functions that probe the relevant forms of translational and orientational order must be introduced. In particular, we measured certain correlation functions that probe the translational ordering of the molecules in an orientationally ordered phase. One of these functions $[g_c(r_\parallel)]$ is sensitive to the stacking of molecules in columns, while another $[g_p(r_\perp)]$ probes the positional ordering of molecules in a plane. In

addition, we measured the correlation functions $g_l(r)$ that probe the spatial correlation of the lth-rank spherical harmonics of the molecular orientation. In addition, we measured orientational order parameters (S and S_c) that probe uniaxial and cubic orientational order. All these probes of liquid-crystalline order are described in more detail in Appendix A.

C. Equation of state

As all our MC "production runs" were performed at constant volume, we needed an efficient technique to measure the pressure in such simulations. To this end, we employed the virtual volume-scaling method that is described in Refs. [3] and [14]. In this method, we perform frequent virtual Monte Carlo steps in which the density is increased by a randomly chosen amount $\Delta\rho$. After such a virtual density increase, we check for overlap of every molecule with its neighbors. We denote the probability that a density increase $\Delta\rho$ will *not* result in an overlap by $P_0(\Delta\rho)$. For not too large values of $\Delta\rho$, $P_0(\Delta\rho)$ is of the form

$$P_0=\exp[-\alpha\Delta\rho+\beta(\Delta\rho)^2+\cdots]\ . \tag{4}$$

For convex molecules, the pressure of the system is related to α, the initial slope of $P_0(\Delta\rho)$, through

$$P=\frac{Nk_BT}{V}\left[1+\frac{\rho\alpha}{2}\right]\ . \tag{5}$$

At sufficiently low densities, our simulation data are in agreement with the prediction based on a five-term virial series. The second virial coefficient of cut spheres is known analytically [10]:

$$B_2=\frac{\pi D^3}{6}\left[\cos\theta_M\left[1+\frac{\sin^2\theta_M}{2}\right]+3\left[\cos\theta_M+\frac{\theta_M\sin\theta_M}{2}\right]\times\left[\cos\theta_M+\frac{\sin^2\theta_M}{2}\right]\right]\ , \tag{6}$$

where $\theta_M\equiv\arccos(L/D)$. We computed B_3 through B_5 numerically. These virial coefficients have been collected in Table I.

TABLE I. Virial coefficients of cut spheres with aspect ratios $L/D=0.1$, 0.2, and 0.3. The second virial coefficient was calculated analytically, using Eq. (6). B_3 through B_5 were calculated using the Monte Carlo procedure of Ree and Hoover [15]. The estimated statistical error in the last digit of the Monte Carlo results is indicated in parentheses.

	$L/D=0.1$	$L/D=0.2$	$L/D=0.3$
B_2/D^3	0.85554	1.08521	1.30052
B_3/B_2^2	0.5084(3)	0.5488(3)	0.5751(2)
B_4/B_2^3	0.1127(4)	0.1715(4)	0.2093(3)
B_5/B_2^4	−0.0101(6)	0.0259(6)	0.0509(4)

D. Determination of first-order-transition densities

In the cut-sphere system, a strong first-order phase transition separates the low-density, translationally disordered phase from the columnar or solid phase. In contrast, the transition between the columnar phase and the crystal appears to be continuous or weakly first order. Similarly, the transition between the isotropic and nematic phase is weakly first order. Standard free-energy calculations [16] can be used to locate the coexistence point in a strong first-order phase transition.

In order for two phases that are separated by a first-order phase transition to coexist, the following equalities must be satisfied:

$$P_{\rm I}=P_{\rm II},\quad G_{\rm I}=G_{\rm II}\ , \tag{7}$$

where P_α is the pressure and G_α the Gibbs free energy of phase α. In practice, we usually compute the Helmholtz free energy F, which is related to G through

$$G=F+PV\ .$$

As the cut-sphere system is athermal, the condition that the temperatures of the two phases must be equal is trivially satisfied and will be disregarded in what follows.

Clearly, knowledge of the pressure and the free energy of both phases is required for the location of the coexistence point. As was explained in Sec. II C, the calculation of the pressure poses no special problems. Once the pressure is known, we can compute the variation of the Helmholtz free energy with density, using the thermodynamic relation:

$$f-f_0=\int_{\rho_0}^{\rho}[P(\rho')/(\rho')^2]d\rho'\ . \tag{8}$$

We use the lowercase f to denote the Helmholtz free energy *per particle*. Equation (8) does not yet allow us to determine the absolute free energy because it contains as an as yet unknown integration constant f_0 the free energy per particle of a reference state at density ρ_0.

In Appendix B, we summarize the approach that we have followed to compute the absolute free energies of the fluid and crystalline phases.

The variation of free energy with density was evaluated analytically by inserting a fit to our equation-of-state data [Eq. (B5)] in Eq. (8). Finally, an iterative search for solutions of Eq. (7) was used to locate the first-order phase-coexistence points (if any).

III. RESULTS FOR CUT SPHERES WITH $L/D=0.1$

A. Introduction

A first numerical study of cut spheres with $L/D=0.1$ was reported by Frenkel [10,11]. These simulations provided strong evidence that cut spheres with $L/D=0.1$ can form four distinct phases: isotropic, nematic, columnar, and solid. One of the main aims of the present paper is to estimate the range of stability of these different phases. In particular, we have applied the techniques described in Appendix B to estimate the location of the

strong first-order transition that separates the nematic and columnar branches of the equation of state.

B. Equation of state

Table II and Fig. 2 show the equation of state of the $L/D=0.1$ system. The data shown in Fig. 2 are based on several series of simulations (both expansion and compression) of a system of 256, 288, and 576 particles that were prepared in different initial condition. In particular, our simulations included the following sequences.

(i) Expansion of the solid phase. This expansion started at $\rho^*=0.90$, where ρ^* is the density relative to the close-packed density.

(ii) Expansion of the nematic phase. This expansion started at $\rho^*=0.38$. The nematic phase was prepared at the latter density by melting a crystal lattice. At a density $\rho^*=0.33$, the system had spontaneously become isotropic.

(iii) Compression of the isotropic phase. The isotropic phase was prepared by melting an overexpanded crystal lattice at a reduced density $\rho^*\approx 0.18$. The system was subsequently compressed slowly beyond the isotropic-metallic transition up to $\rho^*=0.38$. At the latter density the system had spontaneously acquired pronounced nematic order.

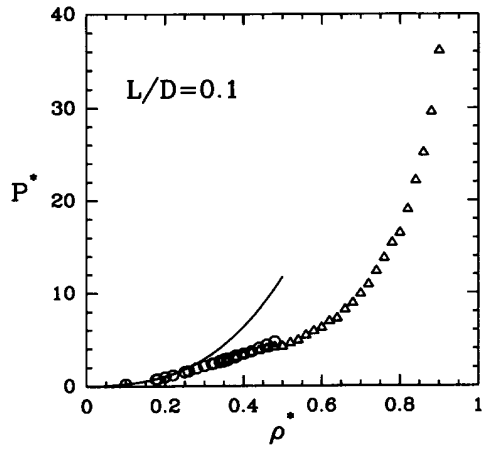

FIG. 2. Equation of state of cut spheres with an aspect ratio $L/D=0.1$. Circles: isotropic-nematic branch. Triangles: columnar-solid branch. The solid line has been computed using a five-term virial series. The pressure is expressed in units of k_BT/D^3, where D is the diameter of a platelet. The unit of density is the density of a cut-sphere crystal at regular close packing [Eq. (3)].

TABLE II. Equation of state for the $L/D=0.1$ system. The data labeled with the superscript(s) were obtained in simulations of $N=256$ particles. The other data on the isotropic branch were obtained using a system of 288 particles. Systems of 576 particles were used in the simulations of the solid and columnar phases. The reduced density is defined as $\rho^*\equiv\rho/\rho_{CP}$, where ρ_{CP} is the density of the crystal at regular close packing. The reduced pressure P^* is defined as Pv_0/k_BT, where v_0 is the volume of a cut sphere: $v_0=(\pi/4)LD^2-(\pi/12)L^3$. The statistical errors are indicated as in Table I.

	Isotropic	Nematic	Columnar-solid	
ρ^*	P^*	P^*	ρ^*	P^*
0.100	0.233(0)$^{(s)}$		0.44	3.73(1)
0.177	0.730(2)$^{(s)}$		0.46	3.96(1)
0.18	0.755(3)		0.48	4.14(1)
0.200	0.948(2)		0.50	4.20(1)
0.22	1.159(4)		0.52	4.57(2)
0.250	1.502(3)		0.54	4.86(2)
0.26	1.603(6)		0.56	5.38(2)
0.28	1.882(3)		0.58	5.84(2)
0.300	2.152(4)		0.60	6.22(2)
0.30	2.145(3)	2.139(8)	0.62	6.92(2)
0.32	2.363(3)	2.370(1)	0.64	7.24(2)
0.325		2.407(5)$^{(s)}$	0.66	8.17(3)
0.34	2.662(3)	2.558(1)	0.68	8.88(3)
0.350	2.834(5)	2.618(5)$^{(s)}$	0.70	9.89(3)
0.350		2.628(5)$^{(s)}$	0.72	10.90(4)
0.36	2.921(4)	2.749(1)	0.74	12.34(8)
0.38	3.210(4)	3.063(1)	0.76	13.77(9)
0.40		3.419(1)	0.78	15.40(8)
0.42		3.665(1)	0.80	16.49(6)
0.44		4.058(1)	0.82	19.02(6)
0.46		4.402(1)	0.84	22.14(8)
0.48		4.746(1)	0.86	25.14(9)
			0.88	29.59(10)
			0.90	36.11(12)

(iv) Compression of a well-aligned nematic phase. This compression was started at a density $\rho^*=0.38$. The system nucleated spontaneously into a structure with columnar order at $\rho^*\approx 0.50$. However, in order to achieve this nucleation, long MC runs (on the order of 2×10^5 trial moves per particle for every state point) had to be performed. We also performed various compression runs on the columnar phase in order to check for hysteresis effects during the columnar-solid transition. No such effects could be observed. The isotropic-nematic transition is expected to be weakly first order, and does indeed show some hysteresis effects. The pressures that we compute are in agreement with the values reported in Ref. [11]. Only at the highest densities on the columnar-solid branch are our values somewhat higher. This difference may be due to the fact that the present runs allowed the initial crystalline lattice more time to equilibrate than the simulations reported in Ref. [11].

C. Phase transitions

1. Columnar-solid transition

Inspection of Fig. 2 shows that there is no direct indication of a solid-columnar transition in the equation of state. This transition can, however, be clearly observed by studying the various pair distribution functions. Figure 3 shows $g(r)$ and $h(z)=g(z)-1$ for densities $\rho^*=0.80$ and 0.54. Figure 4 shows $g_c(r_\parallel)$ and $g_p(r_\perp)$ for the same densities and Fig. 5 shows two corresponding

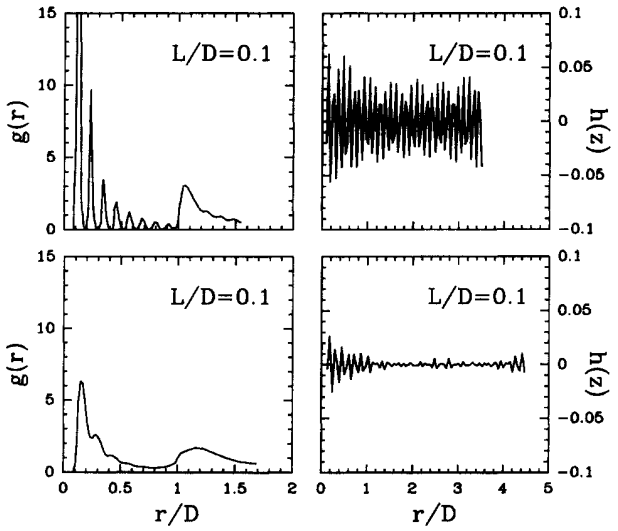

FIG. 3. Left: radial distribution function of a system of cut spheres with aspect ratio $L/D=0.1$ at a density $\rho^*=0.80$ (top) and $\rho^*=0.54$ (bottom). Right: behavior of the correlation function $h(z)\equiv g(z)-1$ at the same densities as the figures on the left. $h(z)$ probes longitudinal density fluctuations. A density $\rho^*=0.80$ corresponds to a state point with crystalline order in the z direction (i.e., along the molecular axes). $\rho^*=0.54$ corresponds to a columnar structure. In that phase, the correlations between particle positions in the z direction are lost. The increase of the oscillations in $h(z)$ for large z is a consequence of the periodic boundary conditions.

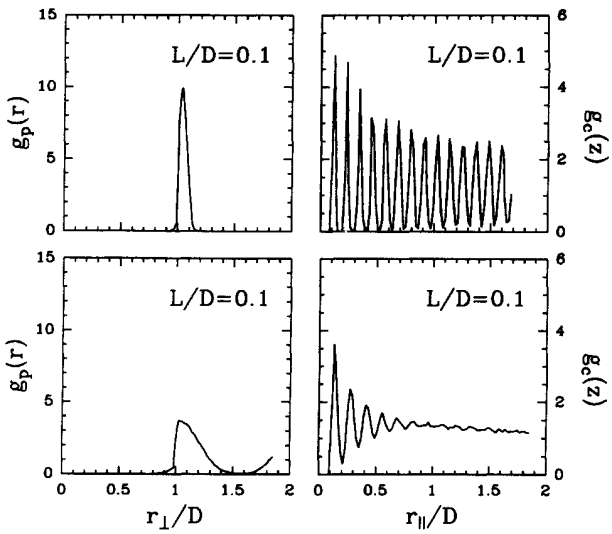

FIG. 4. Pair distribution functions that probe positional order in a direction perpendicular (left) and parallel (right) to the axis of a cut sphere. For a definition of these correlation functions, see Sec. II B. The top two figures were obtained for a system of cut spheres with $L/D=0.1$ at a reduced density $\rho^*=0.80$ (solid phase) and $\rho^*=0.54$ (columnar phase). The figure on the lower right clearly shows the decay of "longitudinal" translational order within one column.

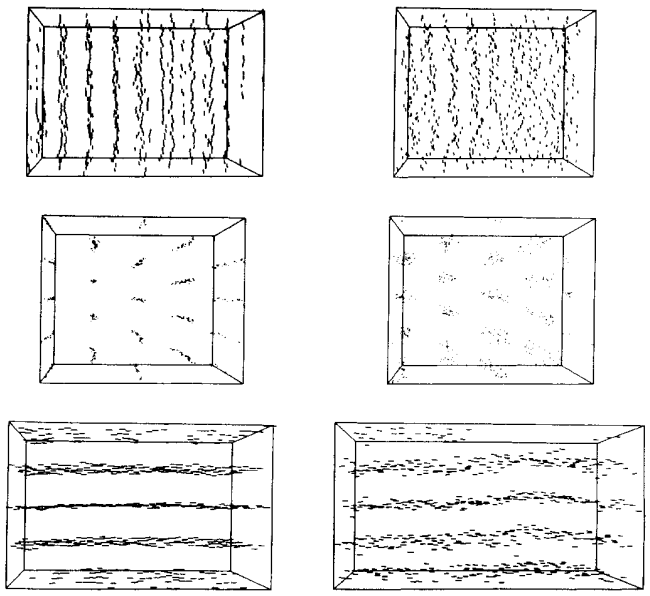

FIG. 5. Configurations of the $L/D=0.1$ system at $\rho^*=0.80$ (left) and $\rho^*=0.54$ (right). At $\rho^*=0.8$, the system is in the crystalline solid phase, whereas it is columnar at $\rho^*=0.54$. Both systems are shown as viewed from three mutually perpendicular directions. In order to be able to see "through" the systems, all cut spheres are represented by line segments of length L along the molecular axis.

configurations. The data were obtained from the series of runs in which the solid phase was expanded. As can be seen from the figures, the system has, in both cases, a hexagonal stacking of columns. However, at $\rho^*=0.54$ the positions of particles both within one column and in different columns are effectively uncorrelated over distances larger than one molecular diameter. Such behavior is to be expected in a columnar phase. Because the particle positions become uncorrelated within a column, this columnar phase is fundamentally different from the one found in small systems of parallel spherocylinders [12]. We have found no evidence for any effect of the system size on the stability of the columnar phase of the system.

It proved difficult to give an accurate estimate of the location of the columnar-solid phase transition on the basis of the available simulation data. The main problem was that, for the system size studied, the crystal-columnar transition appears to be continuous. We therefore tried to locate the transition as the point where the modulation of the longitudinal density-correlation function $h(z)$ becomes long ranged. As the particles in the columnar and crystalline phase have been prepared with their axes aligned to the z axis of the simulation box we can, in this case, use a correlation function that is defined in a reference frame fixed with respect to the simulation box. In order to detect the onset of long-range order in $h(z)$, we fitted its envelope to a function of the form

$$f(z)=a_1\cosh((z-B_z/2)/r_c)+a_2 \ . \tag{9}$$

The functional form of a hyperbolic cosine was chosen because in a periodic system, $f(z)$ should be symmetric around $z=B_z/2$, where B_z is the box length in the z direction. In the fits, we varied the amplitude of the envelope (a_1), the range of the modulation (r_c), and the background level of the modulation (a_2). In the crystalline phase, we expect a_2 to be nonzero, while we should expect the "correlation length" r_c to grow as the phase transition is approached. Indeed, we find that the coefficients a_2 are small [$O(10^{-2})$] for densities less than $\rho^*=0.80$. This suggests that the transition to the crystalline phase takes place at a higher density. However, the errors in the parameters a_1, a_2, and r_c were large and strongly correlated. As a consequence, we could not obtain a more precise indication of the phase transition density. We therefore tentatively identify $\rho^*=0.80$ as a lower limit for the columnar-crystal transition density.

2. *Isotropic-nematic transition*

As mentioned above, the isotropic-nematic phase transition is expected to be weakly first order. In Ref. [4], free-energy calculations were used to estimate the location of the isotropic-nematic (*I-N*) transition of hard ellipsoids. However, the accuracy of this method in locating the *I-N* transition is rather poor. In the present paper we therefore used another less rigorous but hardly less accurate method to locate the *I-N* transition. It is known, both from experiment and from computer simulation (see, e.g., Ref. [3]), that the order parameter S in the nematic phase at the *I-N* transition has a value of 0.3–0.4. Moreover, in the vicinity of this transition, S varies rapidly with density. Hence one way to estimate the location of the *I-N* transition is to determine the point in the nematic phase where $S\approx 0.3$, and assume that this state point coexists with a point on the isotropic branch at the same pressure. In our calculations, we estimated the nematic order parameter in two different ways. In the first method, we looked at the decay of the orientational correlation function $g_2(r)$ (see Sec. II B). In the nematic phase, we have the following relation between S and the behavior of $g_2(r)$ for large r [3]:

$$\lim_{r\to\infty} g_2(r)=S^2 \ . \tag{10}$$

In the second method, we computed S directly from the eigenvalues of the second-rank orientational alignment tensor $\mathbf{Q}$ defined as

$$\langle \mathbf{Q}\rangle=\frac{1}{N}\sum_{i=1}^{N}\langle \tfrac{3}{2}\mathbf{u}_i\mathbf{u}_i-\tfrac{1}{2}\mathbf{I}\rangle \ . \tag{11}$$

The estimate of the nematic order parameter that we have used is

$$S=-2\lambda_0 \ , \tag{12}$$

where λ_0 is the middle eigenvalue of the tensor $\langle \mathbf{Q}\rangle$. As discussed in Ref. [3], Eq. (12) is best suited to estimate the nematic order parameter close to the *I-N* transition. Table III contains the values for S obtained by both methods during a slow expansion of the nematic phase toward the isotropic phase. Of course, $g_2(r)$ cannot be calculated at $r=\infty$, but it is calculated for the largest meaningful distance r that fits within the simulation box. As can be seen from Table III, the variation of S with density is indeed quite steep near the *I-N* transition. The approximate criterion $S_{I\text{-}N}\approx 0.3$–$0.4$ allows us to estimate the density of the nematic phase at the *I-N* transition as $\rho^*_{\text{nem}}=0.335\pm0.005$. We denote that this accuracy is no worse than would have been obtained if the *I-N* transition had been located using the technique described in Ref. [4]. In order to determine the density of the isotropic phase at coexistence we must find the point on the isotropic branch that has the same pressure as $\rho^*_{\text{nem}}=0.335$ on the nematic branch. Using local fits to

TABLE III. Nematic order parameter of a system of cut spheres with aspect ratio $L/D=0.1$. The order parameter was determined both from $g_2(r)$ and from the eigenvalues of the second-rank orientational ordering tensor (see text). $r_{\max}$ is the maximum value of r for which $g_2(r)$ was determined.

ρ^*	$\sqrt{g_2(r_{\max})}$	S
0.30	0.14	−0.04±0.06
0.31	0.00	0.01±0.06
0.32	0.18	0.03±0.06
0.33	0.26	0.05±0.06
0.34	0.58	0.52±0.05
0.36	0.79	0.76±0.03
0.38	0.87	0.87±0.01

TABLE IV. Transition densities for the various phase transitions of cut spheres with aspect ratios $L/D=0.1$, 0.2, and 0.3. The columnar-solid densities are lower bounds. For $L/D=0.2$ two transition densities are given for the cubatic-to-columnar transition, corresponding to the two different fits in Table IX. The statistical errors are indicated as in Table I.

L/D	Transition	ρ^*_{iso}	ρ^*_{cub}	ρ^*_{nem}	ρ^*_{col}	ρ^*_{sol}
0.1	isotropic-nematic	0.330(5)		0.335(5)		
0.1	nematic-columnar			0.497(6)	0.546(10)	
0.1	columnar-solid					0.80
0.2	isotropic-cubatic	0.54–0.57				
0.2	cubatic-columnar (compression)		0.581(10)		0.660(2)	
0.2	cubatic-columnar (expansion)		0.596(10)		0.667(2)	
0.2	columnar-solid					0.73(1)
0.3	isotropic-solid	0.592(2)				0.689(2)

interpolate the equation of state of both the isotropic and nematic branches, we find the isotropic transition density to be $\rho^*_{iso}=0.330\pm0.005$. Note that the density change at the I-N transition is indeed quite small ($\sim 1\%$).

3. *Nematic-columnar transition*

The transition between the nematic and columnar phases is strongly first order. The transition densities were therefore estimated with the aid of the techniques described in Appendix B. For the columnar phase the free energy was calculated in two steps. First, we computed the absolute free energy of the high-density crystalline solid by constructing a reversible path to the corresponding Einstein crystal (see Appendix B). Subsequently, we used thermodynamic integration [Eq. (8)] to compute the free energy along the solid-columnar branch. This procedure implicitly assumes that it is possible to expand reversibly from the solid to the columnar phase. In Sec. III C 1, we have indicated that this is indeed the case.

The free energy of the nematic phase was computed through thermodynamic integration [Eq. (8)] from the ideal-gas phase. This integration path crosses the isotropic-nematic transition. We therefore used Eq. (8) to calculate the Gibbs free energy of the isotropic phase G_I at the I-N coexistence density $\rho^*_I=0.330$. From Sec. III C 2 we know that G_I should be equal to G_N, the Gibbs free energy of the nematic phase at $\rho^*=0.335$. Starting from $\rho^*_N=0.335$, we continue our thermodynamic integration along the nematic branch of the equation of state up to the point where the Gibbs free energy of the nematic phase is equal to that of the columnar phase at the same pressure. In Table IV, we have collected all our data about the location of the phase transitions in a system of cut spheres with $L/D=0.1$.

IV. RESULTS FOR CUT SPHERES WITH $L/D=0.2$

A. Introduction

A first numerical study of cut spheres with $L/D=0.2$ was reported by Frenkel [11]. The results of the latter simulations were quite surprising, as they indicated that the behavior of cut spheres with $L/D=0.2$ differs significantly from that of the corresponding model system with $L/D=0.1$. To be specific, the $L/D=0.2$ system exhibits isotropic, columnar, and solid phases, but it appears to have no stable nematic phase. Instead, the simulations in Ref. [11] provided evidence for the existence of a novel phase with cubic orientational order (cubatic phase). In this section we report a more detailed study of the different phases of the cut-sphere system with $L/D=0.2$. In particular, we have performed extensive calculations to gain a better understanding of the cubatic phase. In addition, we have computed the location of the first-order phase transition from the low-density isotropic-cubatic branch to the columnar-crystalline branch.

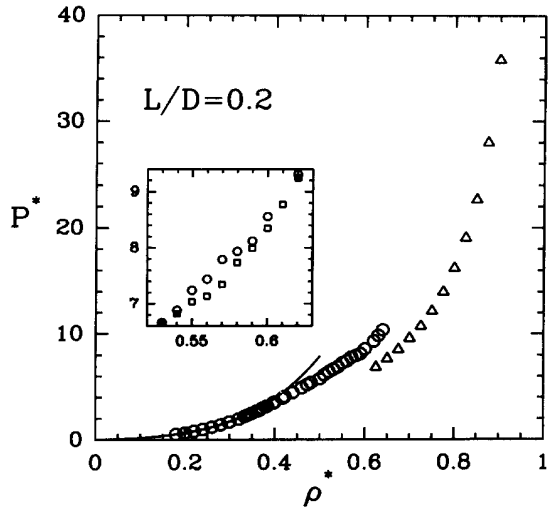

FIG. 6. Equation of state of cut spheres with an aspect ratio $L/D=0.2$. Inset: equation of state for $0.52<\rho^*<0.63$. For the sake of clarity the data points belonging to the cubatic expansion branch are only shown in the inset. Circles: compression; squares: expansion. The presence of a hysteresis loop in the inset suggests that the transition from isotropic to cubatic is weakly first order. The solid line has been computed using a five-term virial series. The pressure is expressed in units k_BT/D^3, where D is the diameter of a platelet. The unit of density is the density of a cut-sphere crystal at regular close packing [Eq. (3)].

B. Equation of state

Figure 6 and Table V show the equation of state of the $L/D=0.2$ system. The data shown in Fig. 6 are based on several series of simulations (both expansion and compression) of systems containing 256, 1728, and 2048 particles. Our simulations included the following sequences.

(i) Compression of an isotropic fluid. In Ref. [11], we have reported the results of compression runs of the isotropic phase of a system of 256 cut spheres, starting at a reduced density $\rho^*=0.20$. These data are shown in

TABLE V. Equation of state of the $L/D=0.2$ system. The compression runs for reduced densities up to $\rho^*=0.50$ were performed on systems of 256 particles. All other results pertain to simulations of systems containing 1728 or 2048 particles. The reduced density is defined as $\rho^*\equiv\rho/\rho_{CP}$, where ρ_{CP} is the density of the crystal at regular close packing. The reduced pressure P^* is defined as Pv_0/k_BT, where v_0 is the volume of a cut sphere: $v_0=(\pi/4)LD^2-(\pi/12)L^3$. The statistical errors are indicated as in Table I.

Isotropic-cubatic			Columnar-solid	
	Compression	Expansion		
ρ^*	P^*	P^*	ρ^*	P^*
0.180	0.508(1)		0.625	6.834(2)
0.199	0.627(1)		0.650	7.637(3)
0.200	0.637(1)		0.675	8.503(3)
0.220	0.788(1)		0.70	9.555(3)
0.240	0.972(1)		0.725	10.716(4)
0.260	1.174(1)		0.75	12.161(4)
0.280	1.412(2)		0.775	13.978(5)
0.298	1.657(4)		0.80	16.205(6)
0.300	1.686(2)		0.825	19.044(7)
0.32		1.945(2)	0.85	22.643(9)
0.333	2.203(5)		0.875	27.988(11)
0.34		2.322(3)	0.90	35.85(2)
0.348	2.463(6)			
0.348	2.467(6)			
0.36		2.692(3)		
0.367	2.804(7)			
0.372	2.963(8)			
0.38		3.111(3)		
0.383	3.162(8)			
0.397	3.47(1)			
0.40	3.531(9)	3.534(3)		
0.417	3.91(1)			
0.42		3.968(3)		
0.422	4.08(1)			
0.44		4.442(4)		
0.447	4.66(2)			
0.447	4.62(2)			
0.46		4.891(4)		
0.472	5.19(2)			
0.48		5.378(5)		
0.497	5.69(2)			
0.50	5.76(2)	5.745(5)		
0.51	6.129(6)			
0.52	6.415(6)			
0.53	6.661(6)	6.647		
0.54	6.881(7)	6.818		
0.55	7.242(7)	7.035		
0.56	7.441(7)	7.133		
0.57	7.789(8)	7.346		
0.58	7.935(8)	7.737		
0.59	8.120(8)	7.990		
0.60	8.557(8)	8.347		
0.61		8.773		
0.62	9.307(7)	9.246		
0.63	9.834(9)			
0.64	10.364(6)			

Table V. In addition, we have performed a series of compression runs on much larger systems ($N=1728$ and 2048), starting from a well-equilibrated isotropic phase at $\rho^*=0.50$. The reason for using much larger system sizes in these runs is that the simulations of Ref. [11] showed that cubatic order develops on compression of the $L/D=0.2$ system at densities above $\rho^*\approx 0.55$. In order to study such ordering in more detail it is clearly important to minimize the effect of the periodic boundary conditions on the phase behavior. In order to equilibrate the system well, extremely long runs are needed (of the order of 10^6 MC trial moves per particle, i.e., a total of some 10^9 trial moves per run).

(ii) Expansion of an isotropic fluid. This expansion started at $\rho^*=0.50$. The data points are in agreement with the results of the compression runs for the smaller ($N=256$) systems.

(iii) Expansion of the cubatic phase. The expansion was started from the cubatic configuration at $\rho^*=0.62$ that was obtained by compression. The expansion runs took about 4×10^4 trial moves per particle for every state point.

(iv) Expansion of a crystalline phase. Here we started with the close-packed lattice structure, at a reduced density of $\rho^*=0.90$. In our simulations we observe the same behavior that was reported in Refs. [10,11], namely, a transition from the crystalline to the columnar phase on expansion along the high-density branch of the equation of state. And, upon compression of the isotropic phase, we observe the spontaneous development of cubic orientational order, extending over the entire simulation box. It is important to stress that the latter ordering transition is not the result of the nucleation of a defect-rich columnar phase from the isotropic fluid. First of all, as will be shown below, the columnar phase itself is not stable at the density where cubic orientational order first sets in. Moreover, by compression and subsequent expansion in a density range $0.55\leq\rho^*\leq 0.59$ it is possible to go from the isotropic to the cubatic phase and back. In fact, in this density range, a hysteresis loop in the pressure is found (see inset of Fig. 6). The occurrence of such a loop may indicate that we are traversing a weak first-order phase transition. Alternatively, the transition could, in fact, be continuous, but the relaxation times in the system are longer than the duration of our runs. Below, we discuss in some detail the nature of the phase with cubic orientational order (cubatic phase).

C. Nature of the cubatic phase

It is important to note that, already in the low-density isotropic phase, there is evidence that the cut spheres tend to assemble spontaneously in short columns. An indication of this is that the radial distribution function develops a peak at short distances ($L<r<2L$). Although the absolute value of this peak is not particularly large in the isotropic phase (typically less than 4), the enhancement over the dilute-gas value of $g(r)$ is quite dramatic. It ranges from a factor of 20 at $\rho^*=0.36$ to almost 3000 at $\rho^*=0.55$ (see Fig. 7). Note that this self-assembly is solely due to excluded volume effects. As the density is

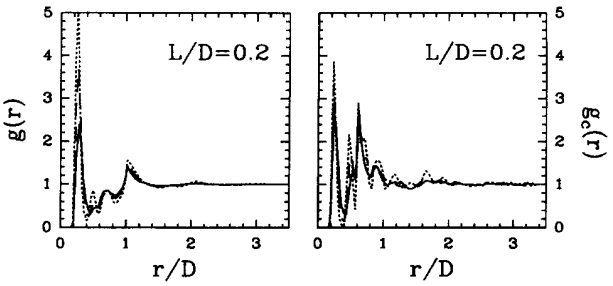

FIG. 7. Radial distribution function $g(r)$ and longitudinal density-correlation function $g_c(r)$ in a cut-sphere system with $L/D=0.2$ at densities $\rho^*=0.51$ (solid line), $\rho^*=0.57$ (long-dashed line), and $\rho^*=0.63$ (short-dashed line). The data are taken from the series of compression runs starting at $\rho^*=0.50$. Note that, at the position of the first peak in $g(r)$, the value of $g(r)$ in the dilute gas is of order 10^{-3}.

increased, the length of these columns grows. However, the columns themselves are orientationally disordered, and hence there is appreciable interaction between different columns. Apparently, this interaction among the columns eventually becomes so severe that the column segments try to order in such a way that the packing problems are minimized. This, in a very qualitative way, describes what happens at the isotropic-to-cubatic transition. In order to find out more about the change in structure that takes place as the system is compressed above $\rho^*=0.55$, it is instructive to look at the various correlation functions that we have defined in Sec. II B. The right-hand side of Fig. 7 shows the density dependence of $g_c(r)$, the function that measures density correlations in a cylinder along the axis of a cut sphere. This function shows very pronounced oscillations at short distances. This is an indication of short-ranged columnar ordering. In fact, this local columnar ordering is much more apparent if we look at $g_c^{\parallel}(r)$ (Fig. 8). Recall

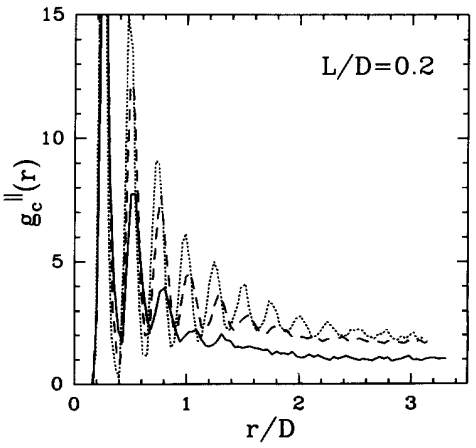

FIG. 8. $g_c^{\parallel}(r)$ in the $L/D=0.2$ system at densities $\rho^*=0.51$ (solid line), $\rho^*=0.57$ (long-dashed line), and $\rho^*=0.62$ (short-dashed line). The data were collected during expansion along the cubatic-isotropic branch. Note that, even at the lowest density ($\rho^*=0.51$), $g_c^{\parallel}(r)$ still shows five peaks. This indicates the presence of short stacks of platelets in the isotropic phase.

that $g_c^{\parallel}(r)$ differs from $g_c(r)$ only in that it ignores positional correlations between cut spheres that are not approximately parallel. This makes $g_c^{\parallel}(r)$ more sensitive to positional correlations of particles that belong to the same column. Indeed, Fig. 8 shows that the number of oscillations in $g_c^{\parallel}(r)$ (which can be considered a rough measure of the number of particles in a column) varies between 5 and 10 as the density is increased from $\rho^*=0.51$ to 0.62. However, although both Figs. 7 and 8 show that the particle positions are strongly correlated over short distances, they also show that this correlation dies out at larger separations. In other words, there is no evidence for any kind of long-range positional ordering in the system.

Next, let us consider the orientational correlations, as measured by the orientational correlation functions $g_l(r)$ [see Eq. (13)]. The density dependence of these correlation functions is shown in Fig. 9. The behavior of these orientational correlation functions is quite striking. First of all, $g_2(r)$ is short ranged in the density range under consideration. This indicates that the system is not forming a nematic phase. However, what we observe is not simply an isotropic fluid. As the system is compressed, $g_4(r)$ and, to a lesser extent, $g_8(r)$ decay increasingly slowly. In fact, at a density above $\rho^*=0.57$, $g_4(r)$ does not decay to zero within half a box diameter. The latter observation indicates that the particles have a tendency to organize in a structure that has cubic orientational ordering extending over at least several molecular diameters. In contrast, $g_6(r)$ decays to zero quickly at all densities. The latter point is important because if the ordering that we observe is simply an artifact due to the periodic boundary conditions, then we should expect to see this in all orientational correlation functions with (even) $l \geq 4$. Figure 10 shows a snapshot of a typical cubatic configuration. This snapshot clearly shows that the

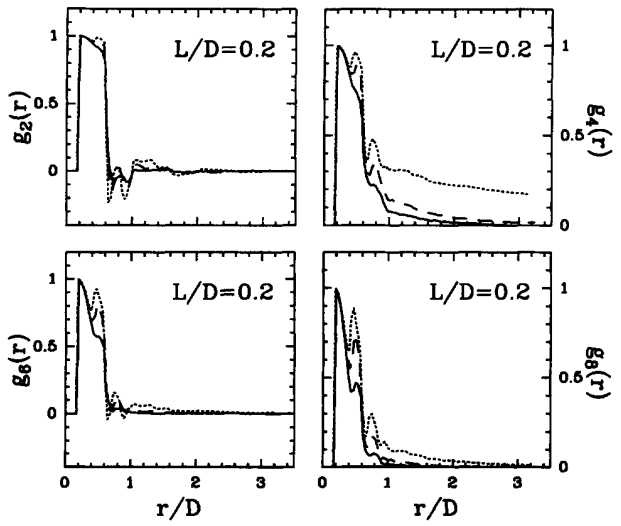

FIG. 9. Orientational distribution functions $g_l(r)$ in the $L/D=0.2$ system. For the definition of these functions, see Eq. (A1). The curves correspond to densities $\rho^*=0.51$ (solid line), $\rho^*=0.57$ (long-dashed line), and $\rho^*=0.63$ (short-dashed line).

FIG. 10. Snapshot of the molecular configuration of a system containing 1728 cut spheres at a reduced density $\rho^*=0.575$. At this density, the range of the cubatic order is comparable to the size of the system. As can be seen from the figure, the platelets spontaneously assemble in short stacks containing four or five particles. Neighboring stacks tend to be approximately perpendicular.

particles tend to align in short columns. Neighboring columns tend to be perpendicular to one another. We find that the length of the columns increases with increasing density until, at $\rho^*\approx 0.60$, some columns become comparable in size to the dimensions of the system (for $N=2048$). Once this happens, the columns tend to align along the box directions. However, at lower densities we do not observe any influence of the orientation of the simulation box on the direction of the columns. This visual observation is confirmed by measurements of the direction of the eigenvector $\mathbf{n}$ of the cubic orientational parameter S_c [see Eq. (14)]. At densities below $\rho^*=0.60$, we found that $\mathbf{n}$ never aligns spontaneously with a box edge. This observation provides additional evidence that the onset of the cubatic order is not due to the periodic boundary conditions.

Information about the nature of the order can be obtained if we consider a log-log plot of $g_4(r)$ vs r (Fig. 11). In this figure, we show the change in $\ln g_4(r)$ as the density is increased from $\rho^*=0.51$ to 0.63. As can be seen in this figure, the cubic orientational order is relatively short ranged for $\rho^* \leq 0.57$. In contrast, for $\rho^* > 0.57$, $g_4(r)$ appears to decay to zero with a power of r, rather than exponentially. It should, however, be stressed that the range over which we can study $g_4(r)$ is quite small. The evidence for a possible algebraic decay of $g_4(r)$ is therefore, at best, suggestive. The density $\rho^*=0.57$, where the cubatic order first extends over the entire system, coincides with the end of the metastable compression branch of the equation of state. Similar behavior is observed upon expansion: here the order becomes short ranged for

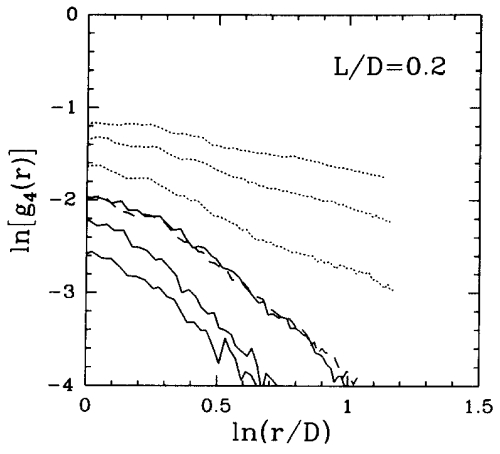

FIG. 11. Double logarithmic plot of $g_4(r)$ vs r, for $\rho^*=0.51$, 0.54, and 0.56 (solid lines), $\rho^*=0.57$ (long-dashed line), and $\rho^*=0.58$, 0.60, and 0.63 (short-dashed lines). These data were collected during a series of slow compression runs starting at $\rho^*=0.50$. The most rapid change in the correlation functions occurs between $\rho^*=0.57$ and 0.58.

$\rho^* \leq 0.54$, at which density the expansion branch of the equation of state joins the compression branch. This behavior suggests that a "weak" first-order phase transition is associated with the onset of cubic orientational order. Very long runs [$O(10^6)$ trial moves per particle] were required to equilibrate the cubatic phase. This suggests that this phase corresponds to a rather glassy state. Table VI shows the density dependence of the cubic orientational order parameter S_c [Eq. (A2)]. The table shows that S_c approaches a value of order 0.5 as the density is increased to $\rho^*=0.6$. However, the change in S_c is not very abrupt. Hence, S_c is not useful as a probe to locate the ordering transition.

TABLE VI. Cubatic order parameter S_c of cut spheres with aspect ratio $L/D=0.2$ and 0.3 as a function of density. The definition of the cubatic order parameter that we have used is given in Eq. (A2). The statistical errors are indicated as in Table I.

ρ^*	S_c
$L/D=0.2$	
0.50	0.086(24)
0.52	0.141(40)
0.54	0.310(21)
0.56	0.441(18)
0.58	0.498(20)
0.60	0.563(18)
$L/D=0.3$	
0.56	0.060(15)
0.58	0.083(17)
0.60	0.113(15)
0.62	0.152(26)
0.64	0.204(12)
0.66	0.294(13)

D. Phase transitions

1. Isotropic-cubatic transition

As stated above, the isotropic-cubatic transition appears to be weakly first order. The transition densities can, however, not be determined easily. The standard method of thermodynamic integration cannot be applied because there is no obvious reversible route from the cubatic phase to any known reference system. The cubatic parameter S_c also does not provide any sharp indication of a transition. Fitting $\log g_4(r)$ to r does shows a fairly abrupt change in the orientational correlation length: both during expansion and compression, this correlation length is of $O(D)$ on the isotropic branch and comparable to the dimension of the simulation box on the cubatic branch. Of course, in the latter case, fitting $g_4(r)$ to an exponential may no longer be meaningful, as the decay $g_4(r)$ appears to be algebraic. In these cases, our estimate of a lower limit for the correlation length is based on a fit of an exponential to $g_4(r)$ at large r. In any event, the range of the orientational order exhibits hysteresis on compression and expansion over the same density range as the equation of state (see the inset in Fig. 6). Therefore, all the available data only allows us to bracket the isotropic-cubatic phase transition in a density range between $\rho^*=0.54$ and 0.57.

2. Solid-columnar phase transition

As in the system of cut spheres with $L/D=0.1$, we did not see any sign of the columnar-to-solid transition in the equation of state. This suggests that this transition is either continuous or weakly first order. We therefore used the same approach as described in Sec. III C 1 to locate this transition. To this end, we fitted the envelope $h(z)$ to f_z of [Eq. (9)]. We find that the coefficient a_2, which is a measure for the degree of long-range columnar order, decreases rapidly when the density is decreased below $\rho^*=0.80$. A linear extrapolation of a_2 vs ρ^* yields $a_2=0$ at $\rho^*=0.76$. Indeed, below this density, a_2 is always found to be very small.

3. Columnar-isotropic transition

As we cannot locate the transition from the isotropic to the cubatic phase accurately, we also have a problem in determining the (strongly first-order) transition between the columnar phase and the isotropic or cubatic phase. In order to arrive at upper and lower bounds for the transition densities, we have made two different fits to the isotropic-cubatic branch of the equation of state. The first fit used the pressure data of the (partly metastable) isotropic branch while the second fit used the data that pertain to the (partly metastable) cubatic branch. Using these two fits, we obtain two different estimates for the location of the transition from the isotropic-cubatic phase to the columnar phase. The real transition densities should be somewhere between these two limits. It turns out that the two estimates are, in fact, not very different. We therefore have used the average of these two esti-

mates as our best estimate of the transition from the isotropic-cubatic branch ($\rho^*=0.59$) to the columnar-solid branch ($\rho^*=0.66$).

As indicated in Appendix B, the free energy of the low-density branch was computed by thermodynamic integration starting from the ideal-gas reference state. An additional free-energy calculation is needed to compute the absolute free energy of the columnar-crystal branch. As before, we used an Einstein crystal as a reference system for the crystalline phase and used thermodynamic integration to compute the free energy along the columnar branch.

Our best estimates for all phase transition densities in the $L/D=0.2$ system have been collected in Table IV. As can be seen from Table IV, the transition to the columnar phase occurs at a density on the isotropic-cubatic branch where the isotropic phase is no longer metastable. This observation is important because it indicates that, for cut spheres with $L/D=0.2$, there is a (narrow) density range where the cubatic phase is thermodynamically stable.

V. RESULTS FOR CUT SPHERES WITH $L/D=0.3$

One of the main surprises of the preceding section was that cut spheres with an aspect ratio $L/D=0.2$ appear to exhibit a stable phase that is characterized by extended (although not necessarily long-ranged) cubic orientational order. It is, of course, of considerable interest to know how the stability of such a phase depends on the aspect ratio of the constituent molecules. From Sec. III we know that cut spheres with $L/D=0.1$ form a nematic rather than a cubatic phase. In the present section we show what happens as the aspect ratio is made larger than 0.2.

Equation of state

The simulations for $L/D=0.3$ were performed on a system of 2048 particles. The equation of state is shown in Fig. 12. In Table VII, we have collected all data points

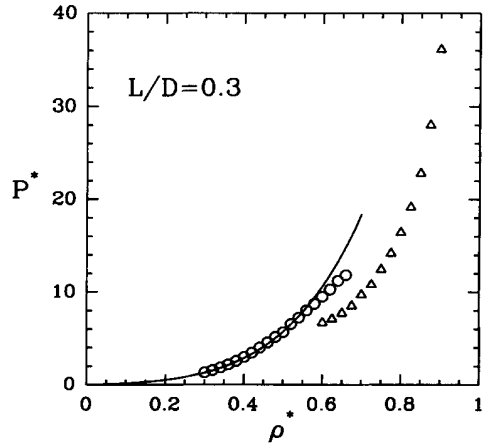

FIG. 12. Equation of state of cut spheres with an aspect ratio $L/D=0.3$. The solid line has been computed using a five-term virial series. The pressure is expressed in units of k_BT/D^3, where D is the diameter of a platelet. The unit of density is the density of a cut-sphere crystal at regular close packing [Eq. (3)].

TABLE VII. Equation of state of the $L/D=0.3$ system. All results were obtained in simulations of systems containing 2048 particles. The reduced density is defined as $\rho^*\equiv\rho/\rho_{CP}$, where ρ_{CP} is the density of the crystal at regular close packing. The reduced pressure P^* is defined as Pv_0/k_BT, where v_0 is the volume of a cut sphere: $v_0=(\pi/4)LD^2-(\pi/12)L^3$. The statistical errors are indicated as in Table I.

Isotropic		Solid	
ρ^*	P^*	ρ^*	P^*
0.30	1.3314(5)	0.60	6.691(3)
0.32	1.5769(6)	0.625	7.101(3)
0.34	1.8616(9)	0.65	7.722(4)
0.36	2.186(1)	0.675	8.509(4)
0.38	2.557(1)	0.70	9.697(5)
0.40	2.978(1)	0.725	10.788(6)
0.42	3.452(2)	0.75	12.435(7)
0.44	3.983(2)	0.775	14.176(8)
0.46	4.546(2)	0.80	16.408(10)
0.48	5.144(3)	0.825	19.134(13)
0.50	5.664(3)	0.85	22.798(16)
0.52	6.528(3)	0.875	28.000(21)
0.54	7.238(3)	0.90	36.111(30)
0.56	8.027(4)		
0.58	8.736(4)		
0.60	9.501(4)		
0.62	10.284(5)		
0.64	11.214(5)		
0.66	11.834(6)		

of our simulations. All results for the $L/D=0.3$ system were obtained in two series of runs, namely, a compression run of the isotropic phase and an expansion run of the crystalline phase. We find that the system has an isotropic, a solid, and possibly a cubatic phase. However, the latter phase is not thermodynamically stable. Moreover, for cut spheres with $L/D=0.3$, we do not observe the formation of a columnar phase, although we do see appreciable disorder in the expanded solid.

Using the techniques described in Appendix B, we are able to locate the first-order phase transition between the isotropic fluid and the crystalline solid. As can be seen in Table IV, there is a strong first-order phase transition from the isotropic fluid at $\rho^*\approx0.6$ to the crystalline solid at $\rho^*\approx0.7$. The isotropic-solid transition occurs before there is any strong tendency toward cubatic ordering in the isotropic phase (see Table VI). We therefore conclude that the $L/D=0.3$ system has no stable cubatic phase.

VI. SUMMARY AND DISCUSSION

In this paper we have studied the phase behavior of a model for disklike mesogens, namely, a system consisting of cut spheres of varying thickness. We find that this model displays a rich phase behavior. The range of stability of the various phases in this model is strongly dependent on the aspect ratio of the particles. For $L/D=0.1$ we find stable isotropic, nematic, columnar, and solid phases, for $L/D=0.2$ we find isotropic, columnar, and solid phases, while for $L/D=0.3$ we only find stable isotropic and solid phases. The fact that we observe columnar ordering in relatively large systems of cut

spheres ($N=576$ for $L/D=0.1$ and $N=2048$ for $L/D=0.2$) makes it plausible that this is indeed a thermodynamically stable phase. In this context it is interesting to note that Azzouz *et al.* have found that there is no columnar phase in a system of 2500 *parallel* cut spheres with aspect ratio $L/D=0.1$ [17]. Apparently, orientational freedom stabilizes the columnar phase of cut spheres. Why this should be so is not intuitively clear.

Most interestingly, our results for cut spheres with $L/D=0.2$ strongly suggest that the cubatic phase reported earlier in Refs. [10,11] may, in fact, be thermodynamically stable in a narrow density range. In this phase, the system has no translational order, but appreciable cubic orientational order (possibly quasi-long-ranged or even long-ranged). We have summarized our knowledge of the phase behavior of the cut-sphere system in a tentative phase diagram (Fig. 13). In fact, we know a few features of this phase diagram for both larger and smaller values of L/D. In particular, we know that for $L/D=1$ (hard spheres), the two-phase region is located between $\rho^*=0.67$ and 0.74. For $L/D\to 0$, the isotropic-nematic transition occurs at $\rho^*=0$.

Of all the phases shown in this phase diagram, the cubatic phase merits special attention because it is different from all known liquid-crystalline phases, although the concept of a phase with such order is not new. In fact, the existence of phases with cubic orientational order has been predicted by Nelson and Toner [18] in a quite different context. In the Nelson-Toner (NT) theory, cubic bond-orientational order without translational order can occur in a solid phase containing free dislocation loops. These dislocation loops cause the elastic constants to become zero, but a finite resistance to torsion remains,

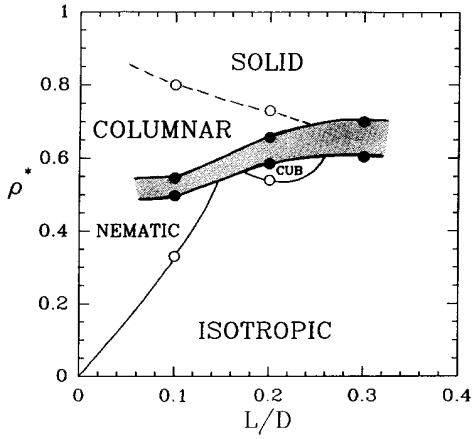

FIG. 13. Tentative phase diagram of cut spheres with an aspect ratio L/D between 0.1 and 0.3. The high-density solid-columnar phase is separated by a first-order phase transition from the low-density fluid phase. The shaded area indicates the two-phase region. The densities of the coexisting phases are indicated by closed circles. The open circles indicate the approximate location of phase transitions that have been estimated using techniques other than free-energy calculations. The isotropic-nematic transition is weakly first order. The same appears to be the case with the isotropic-cubatic transition. In our simulations, the transition between the solid and the columnar phases appeared to be continuous.

thus distinguishing this phase from an isotropic phase. In the NT theory, the solid-to-cubatic transition is predicted to be either continuous or weakly first order. It should be stressed that the NT theory was formulated for atomic solids. Hence, it is not obvious if the NT theory would apply to the cubatic phase reported in the present work.

We should also point out that there is still another phase that has cubic orientational order but no translational order. This phase was first discussed by one of us in the context of the Onsager model for the isotropic-nematic transition [11]. In Ref. [11] it is argued that particles consisting of three mutually perpendicular thin hard rods *must* form a phase with long-range cubic orientational order at sufficiently high density (although still at a vanishingly small volume fraction). However, the local structure of such a very dilute cubatic phase is expected to be completely different from the one considered above.

At this stage, we can only speculate about the factors that favor extended cubic orientational ordering in a system of cut spheres. First of all, we note that even in the isotropic phase there is a tendency for molecules to assemble in short columns. As the density is increased, one might expect these columns to grow without bound. However, this is not likely for the following reason: consider what happens if we compress a fluid of disklike particles. The molecules will aggregate in columns to increase their total free volume, at the expense of some translational and orientational entropy. However, after the length of a column has become comparable to the diameter of a platelet, there is no great advantage to add the next platelet to the top or bottom of the column, rather than to the sides. In other words, we expect that the columns will start to sprout mutually perpendicular branches. If this occurs, we should expect to see enhanced cubic order, at least locally. It is also possible to approach the same problem from another point of view, namely, that as the columns grow, their mutual steric hindrance increases rapidly. This approach has recently been explored by Michels and Hendriks [19].

If we approach the problem of cubatic ordering from the solid side, it is most instructive to consider a crystal of square "tiles" with a rational aspect ratio. Such a model will have a strongly degenerate close-packed structure. In this disordered solid the molecules are orientationally ordered, but their centers-of-mass are translationally disordered. In fact, the existence of a similar stable, translationally disordered solid structure has recently been demonstrated in the case of a two-dimensional model by Wojciechowski, Frenkel, and Branka [20]. It seems plausible that, as a three-dimensional solid of square tiles is expanded, cubic orientational order will survive all the way down to the melting point. Of course, the model considered in the present paper is different from the square-tile system. Yet it should be possible to pack cut spheres in fairly dense, translationally disordered structures with cubic orientational order. Of course, at very high densities, the close-packed structure of the cut-sphere system will always be most stable. However, it seems likely that once this structure melts, the system will organize into a structure that resembles,

at least locally, the disordered structure of the square-tile system.

The above arguments all suggest that it is advantageous for cut spheres to form a phase with appreciable *local* cubic order. But neither provides any explanation for *(quasi-)long ranged* orientational order. It should however be stressed that our simulations cannot provide any conclusive information about the orientational order on macroscopic length scales. The present simulations have been performed on model systems that are about as large as can be conveniently equilibrated with present-day computers (recall that in the cubatic regime, one single run typically required 10^8 MC trial moves). However, in order to perform a systematic study of the isotropic-cubatic transition, a finite-size scaling analysis of the simulation results would be needed. Such an analysis would require simulations of systems that are about ten times larger than what we could study. In view of the extreme sluggishness of the system in the cubatic phase, such simulations would probably require about a factor of 10^3 more computer power than we can afford at present. In any case, it is important to realize that a phase with only local cubic orientational order would have the same symmetry as the low-density isotropic phase and may therefore be separated from the latter by a first-order phase transition. The question about the *range* of the cubatic order is therefore separate from the question about the *existence* of a phase with such order, be it local or global.

Finally, we should note that, to our knowledge, no phase with (local) cubic orientational order has been observed experimentally. It is therefore of considerable interest to know how a cubatic phase, if it occurs in nature, could be observed experimentally. For most experimental probes it makes a large difference whether the cubic orientational order is local or (quasi-)long-ranged. In the latter case, x-ray diffraction could be used to study the scattering by a cubatic "single crystal". However, even if cubatic order is long ranged, it is not at all clear if and how sufficiently large single-domain samples could be prepared. Most other techniques that could probe cubatic order suffer from the same drawback that they require single-domain samples. For this reason, a real-space technique that directly probes the local molecular configuration seems much more promising, first of all because it would not require the preparation of large single domains, but most importantly, because such a direct technique could also detect cubatic order, even if it turns out that the latter is not long ranged.

ACKNOWLEDGMENTS

We thank Evert Jan Meijer and Bela Mulder for a critical reading of the manuscript. The work of the FOM Institute is part of the research program of FOM (Stichting Fundamenteel Onnderzoek der Materie) and is supported by the Nederlandse Organisatie voor Wetenschappelijk Onderzoek (NWO).

APPENDIX A: PROBES OF LIQUID-CRYSTALLINE ORDER

Below, we describe the different structural probes that we have measured during our MC simulations of the cut-sphere system.

1. Translational correlation functions

In addition to the usual radial distribution function $g(r)$, we measured several functions that probe anisotropic density correlations. Simplest among these functions is the longitudinal density-correlation function denoted by $g(z)$. This function measures the amplitude of density correlations in the direction of the initial alignment of the molecules. In simulations that start from a well-ordered crystal lattice, the alignment direction is imposed and it is retained when the system is subsequently slowly equilibrated and expanded. However, $g(z)$ becomes useless as a probe when the system undergoes an orientational disordering transition on expansion. Similarly, configurations that have been generated by compression from the isotropic phase will not usually align spontaneously along the z axis. In that case too, a function such as $g(z)$ that measures directional correlations in a frame fixed by the orientation of the simulation box is not a suitable probe. We have therefore introduced a number of correlation functions that measure spatial correlations of the density or the molecular orientation in a molecule-fixed frame. Below, we describe several correlation functions that can be used to probe density correlations in directions parallel and perpendicular to the axis of individual molecules. Let us first consider the correlation functions that probe transverse density correlations (i.e., in a direction perpendicular to the molecular axis). The simplest function to measure such correlations is denoted by $g(r_\perp)$. Here $r_\perp$ is defined as the component of the distance between two particles perpendicular to the orientation of one particle. $g(r_\perp)$ can, for instance, be used to distinguish a columnar phase, where the ordering of columns in a two-dimensional crystal lattice creates a strong modulation of $g(r_\perp)$, from a nematic phase, where $g(r_\perp)$ is rather featureless. A function closely related to $g(r_\perp)$ is $g_p(r_\perp)$. The latter function probes transverse positional correlations with other molecules that have their centers of mass in a slab within $L/2$ from the equatorial plane of the molecule at the origin of our coordinate frame (of course, in computing this correlation function, we average the correlations measured in all distinct molecule-fixed coordinate frames). In our simulations, it turned out that $g(r_\perp)$ and $g_p(r_\perp)$ yielded very similar information. For this reason, we only show the results for $g_p(r_\perp)$.

In order to probe the onset of columnar order, it is also convenient to measure longitudinal density correlations in a molecule-fixed frame. To this end, we defined two closely related functions: $g_c(r_\parallel)$ and $g_c^{\parallel}(r_\parallel)$ (the subscript c stands for cylinder, as will be explained below). Both functions measure density correlation in a direction along the molecular axis ($r_\parallel$). Both $g_c(r_\parallel)$ and $g_c^{\parallel}(r_\parallel)$ count correlations with particles that lie within a cylinder of diameter D along the axis of the reference molecule. How-

ever, in $g_c^{\parallel}(r_{\parallel})$ we only "count" a molecule if it is aligned to within 30° with the reference molecule. These functions proved to be very sensitive to the appearance of local columnar order in the system.

2. Orientational correlation functions

In order to probe possible orientational ordering in a system we measured the orientational correlation functions $g_l(r)$, defined as

$$g_l(r)=\langle P_l(\mathbf{u}(0)\cdot\mathbf{u}(r))\rangle \ , \tag{A1}$$

where $P_l(x)$ is the lth Legendre polynomial and $\mathbf{u}(r)$ is a unit vector along the axis of the molecule at distance r from the reference molecule. We have measured $g_l(r)$ with $l=2$, 4, 6, and 8. In the nematic phase all these functions are long ranged. In the isotropic phase they decay to zero within one molecular diameter.

3. Order parameters

In order to distinguish between phases with different symmetry, it is convenient to measure characteristic order parameters that vanish in one phase, but not in the other. In order to study the onset of orientational order we measured the nematic order parameter S. This parameter was determined as described in Ref. [3] [see Eqs. (11) and (12) in Sec. III C 1]. We also defined an order parameter S_c that provides a measure for the degree of orientational order with cubic symmetry:

$$S_c \equiv \max_{\mathbf{n}} \frac{12}{7}\frac{1}{N}\sum_{i=1}^{N}\langle P_4(\mathbf{u}_i\cdot\mathbf{n})\rangle \ . \tag{A2}$$

Here $P_4(z)$ is the fourth Legendre polynomial, N is the number of particles, $\mathbf{u}_i$ is a unit vector along the symmetry axis of a cut sphere, and the unit vector $\mathbf{n}$ is chosen such that it maximizes S_c. The angular brackets denote an ensemble average. The factor $\frac{12}{7}$ has been included to ensure that $S_c=1$ for a system with perfect cubic orientational order. For nematic order, S_c can become greater than 1. Of course, other definitions of a cubic orientational order parameter are possible [21]. However, Eq. (A2) has the advantage that it provides information both about the magnitude of P_4 and about the vector(s) $\mathbf{n}$, for which the maximum of P_4 occurs, i.e., the space-fixed coordinate frame in which the orientational order is maximal.

Additional information about the structure of the various phases of the cut-sphere system was obtained from direct inspection of snapshots of the molecular configurations.

APPENDIX B: LOCATION OF FIRST-ORDER PHASE TRANSITIONS

In this appendix, we discuss how the free energy of the fluid and solid phases of our model system is related to the free energy of a known reference state.

For the isotropic phase, a convenient choice for the reference state is the ideal gas for which f_0 is known analytically. No such simple reference state exists for the solid phase of a hard-core system. We therefore use an artificial thermodynamic integration procedure to relate the free energy f_0 of the solid at a particular density ρ_0 to the free energy of an Einstein crystal of the same structure, at the same density [13]. The potential energy of this reference Einstein crystal is given by

$$U_E(\lambda_1,\lambda_2)=\lambda_1\sum_{i=1}^{N}\Delta\mathbf{r}_i^2+\lambda_2\sum_{i=1}^{N}\sin^2\theta_i \ , \tag{B1}$$

where $\Delta\mathbf{r}_i\equiv\mathbf{r}_i-\mathbf{r}_i^0$ and θ_i denote, respectively, the translational and angular displacement of particle i from its equilibrium position and orientation. λ_1 and λ_2 are the coupling parameters which determine the strength of the harmonic force. The Einstein crystal is a convenient reference system, because its free energy per particle is known in closed form. For large values of the coupling constants the configurational part of this free energy is approximately given by

$$f_E\approx-\frac{k_BT}{N}\ln\left[N^{-3/2}\left[\frac{\pi}{\beta\lambda_1}\right]^{3/2(N-1)}\left[\frac{2\pi}{\beta\lambda_2}\right]^{N}\right] \qquad (\lambda_{1,2}\to\infty) \ , \tag{B2}$$

where we have imposed the additional constraint that the center of mass of the system is kept fixed. In order to construct a reversible path from the Einstein crystal to a cut-sphere crystal at the same density, we introduce a generalized potential-energy function U_{λ_1,λ_2}

$$U_{\lambda_1,\lambda_2}=U_0+U_E(\lambda_1,\lambda_2) \ , \tag{B3}$$

where U_0 is the potential-energy function of the cut-sphere system in the absence of any harmonic springs. For sufficiently large values of λ_1 and λ_2, the free energy of this interacting Einstein crystal reduces to the free energy of the ideal Einstein crystal. This equality only holds if all configurations of the ideal Einstein crystal are also acceptable configurations of the interacting system. In practice, a small fraction P_0 of the configurations of the ideal Einstein crystal would result in hard-core overlaps. However, it is easy to correct for this effect [13]. In order to compute the free energy f_0 of the cut-sphere system at the reference state ρ_0, we perform thermodynamic integration to compute the change in free energy as we slowly switch off the Einstein crystal coupling constants λ_1 and λ_2 from their maximum value $\lambda_{1,2}^{\max}$. The final expression that relates f_0 to the free energy of the ideal Einstein crystal is [13]

TABLE VIII. Free energy per particle of the solid phase (f_s) of cut spheres with $L/D=0.1$, 0.2, and 0.3. The reference state for the free energy has been chosen such that the absolute free energy per particle of an ideal gas at density ρ is given by $f_{id}/(k_BT)=[\ln\rho-1-\ln(4\pi)]$. The statistical errors are indicated as in Table I.

L/D	ρ_s^*	f_s
0.1	0.80	14.38(4)
0.2	0.80	12.39(2)
0.3	0.80	11.07(2)

TABLE IX. Coefficients of the y expansion of the equation-of-state data. Column 3 gives the range of validity of the expansion. Note that we have included fits to the equation of state of the isotropic phase, starting at a finite density. At lower densities, the equation of state of the isotropic phase was adequately described by a five-term virial series (see Table I).

L/D	Phase	ρ^*	C_1^*	C_2^*	C_3^*	C_4^*	C_5^*
0.1	isotropic	0.10–0.33	0.2359	23.486	−23.562		
0.1	nematic	0.335–0.48	5.233	1.2455			
0.1	columnar	0.44–0.90	7.808	−5.976	4.507	−1.233	0.119
0.2	isotropic-cubatic (compression)	0.18–0.64	0.224	11.408	7.028	−19.638	8.272
0.2	isotropic-cubatic (expansion)	0.20–0.64	0.846	5.933	22.954	−37.824	15.182
0.2	columnar-solid	0.62–0.84	4.902	0.127	0.156		
0.3	isotropic	0.30–0.66	−1.0550	14.819	−5.8156		
0.3	solid	0.60–0.90	5.714	−0.419	0.288		

$$f_0=f_E(\lambda_1^{\max},\lambda_2^{\max})+\frac{k_BT}{N}P_0-k_BT\frac{\ln V}{N}-\int_0^{\lambda_1^{\max}}d\lambda_1\langle\Delta r^2\rangle_{\lambda_1,\lambda_2}-\int_0^{\lambda_2^{\max}}d\lambda_2\langle\sin^2\theta\rangle_{\lambda_1,\lambda_2}\,, \tag{B4}$$

where $\langle\Delta r^2\rangle_{\lambda_1,\lambda_2}$ is the mean-square displacement of a particle from its lattice site at a given value of λ_1 and λ_2 and at a fixed center of mass. The term $(-k_BT\ln V)/N$ corrects the free energy for this fixed center-of-mass constraint. Of course, the thermodynamic integration to the Einstein crystal must be performed at a density where the crystalline phase is at least mechanically stable.

In Table VIII, we have collected our results for the free-energy calculations of the solid phase of cut spheres with $L/D=0.1$, 0.2, and 0.3. All these calculations were performed at a density corresponding to 80% of regular close packing.

Once the absolute free energy of a phase is known at one density, we can use Eq. (8) to compute it at any other density that can be reached by reversible expansion or compression from the reference state. In practice, Eq. (B4) was integrated using a ten-point Gauss-Legendre quadrature. In order to compute the variation of the free energy with density the equation-of-state data were fitted to an analytical function of the form [22]:

$$P^*(\rho)=\sum_n C_n^* y^n\,, \tag{B5}$$

where $P^*=Pv_0/k_BT$, with v_0 the volume of a particle, and

$$y=\frac{v_0\rho}{1-v_0\rho}\,. \tag{B6}$$

This functional form of the equation of state is known under the name y expansion. In Ref. [22] this functional form is introduced as an improvement over the virial series in describing the equation of state of moderately dense molecular fluids. In the present work we have used the y expansion simply as a convenient function to fit our data. In particular, we have also used it in the solid and columnar phase. We stress that in such ordered phases, the y expansion is no more fundamental than any other functional form that fits the data. The results of all our y-expansion fits have been collected in Table IX.

*Present address: Buys-Ballotlaboratorium, Rijksuniversiteit Utrecht, P. O. Box 80 000, 3508 TA Utrecht, The Netherlands.

[1] M. P. Allen, D. Frenkel, and J. Talbot, J. Comput. Phys. Rep. **9**, 301 (1989).
[2] A. Stroobants, H. N. W. Lekkerkerker, and D. Frenkel, Phys. Rev. A **36**, 2929 (1987).
[3] R. Eppenga and D. Frenkel, Mol. Phys. **52**, 1303 (1984).
[4] D. Frenkel and B. M. Mulder, Mol. Phys. **55**, 1171 (1985).
[5] M. P. Allen, Phys. Rev. Lett. **65**, 2881 (1990).
[6] J. Wesemann, L. Qin, and P. Siders, Langmuir **5**, 1358 (1989); M. He and P. Siders, J. Phys. Chem. **94**, 7280 (1990).
[7] M. C. Duro, J. A. Martin-Pereda, and L. M. Sesé, Phys. Rev. A **37**, 284 (1988).
[8] M. Wojcik and K. E. Gubbins, Mol. Phys. **53**, 397 (1984).
[9] See, e.g., P. S. Pershan, *Structure of Liquid Crystal Phases* (World Scientific, Singapore, 1988).
[10] D. Frenkel, Liq. Cryst. **5**, 929 (1989).
[11] D. Frenkel, in *Liquids, Freezing and the Glass Transition,* edited by J. P. Hansen and D. Levesque (North-Holland, Amsterdam, 1991), p. 691.
[12] J. A. C. Veerman and D. Frenkel, Phys. Rev. A **43**, 4334 (1991).
[13] D. Frenkel and A. J. C. Ladd, J. Chem. Phys. **81**, 3188 (1984).
[14] D. Frenkel, in *Computer Modelling of Fluids, Polymers and Solids,* edited by C. R. A. Catlow, S. C. Parker, and M. P. Allen (Kluwer Academic, Dordrecht, 1990), p. 83.
[15] F. H. Ree and W. G. Hoover, J. Chem. Phys. **49**, 639 (1964).
[16] See, e.g., D. Frenkel, in *Molecular-Dynamics Simulation of Statistical Mechanical Systems,* edited by G. Ciccotti and W. G. Hoover (North-Holland, Amsterdam, 1986), p. 151.

[17] H. Azzouz, J. M. Caillol, D. Levesque, and J. J. Weis (unpublished).
[18] D. R. Nelson and J. Toner, Phys. Rev. B **24**, 363 (1981).
[19] M. A. J. Michels and E. M. Hendriks (unpublished).
[20] K. W. Wojciechowski, D. Frenkel, and A. C. Branka, Phys. Rev. Lett. **66**, 3168 (1991).
[21] M. V. Jarić, Nucl. Phys. B **265**, 647 (1986).
[22] B. Barboy and W. M. Gelbart, J. Chem. Phys. **71**, 3053 (1979).

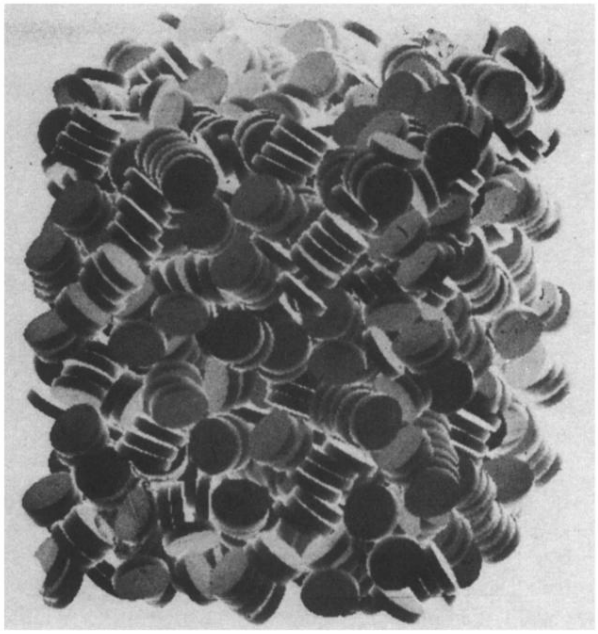

FIG. 10. Snapshot of the molecular configuration of a system containing 1728 cut spheres at a reduced density $\rho^* = 0.575$. At this density, the range of the cubatic order is comparable to the size of the system. As can be seen from the figure, the platelets spontaneously assemble in short stacks containing four or five particles. Neighboring stacks tend to be approximately perpendicular.

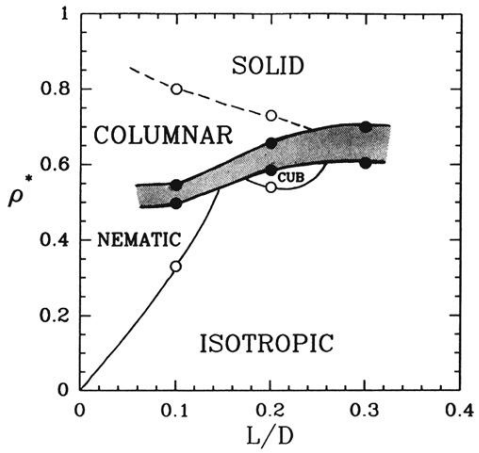

FIG. 13. Tentative phase diagram of cut spheres with an aspect ratio L/D between 0.1 and 0.3. The high-density solid-columnar phase is separated by a first-order phase transition from the low-density fluid phase. The shaded area indicates the two-phase region. The densities of the coexisting phases are indicated by closed circles. The open circles indicate the approximate location of phase transitions that have been estimated using techniques other than free-energy calculations. The isotropic-nematic transition is weakly first order. The same appears to be the case with the isotropic-cubatic transition. In our simulations, the transition between the solid and the columnar phases appeared to be continuous.